How do host population dynamics impact Lyme disease risk dynamics in theoretical models?

Joseph D.T. Savage[1,2*], Christopher M. Moore[1]

[1] Biology Department, Colby College, Waterville, Maine, United States of America

[2] Graduate Program in Ecology, Evolution, Environment, and Society, Department of Geography, Dartmouth College, Hanover, New Hampshire, United States of America

[*] Corresponding Author

Email: joseph.d.savage.gr@dartmouth.edu (JDTS)

1 Abstract

Lyme disease is the most common wildlife-to-human transmitted disease reported in North America. The study of this disease requires an understanding of the ecology of the complex communities of ticks and host species involved in harboring and transmitting this disease. Much of the ecology of this system is well understood, such as the life cycle of ticks, and how hosts are able to support tick populations and serve as disease reservoirs, but there is much to be explored about how the population dynamics of different host species and communities impact disease risk to humans. One way in which we can study disease effectively is through the use of theoretical models. These are powerful tools that allow investigation of complex species interactions before staging complicated and expensive studies that may not be productive. We construct a model to investigate how host population dynamics can affect disease risk to humans. The model describes a tick population and a simple community of three species in which mouse populations are made to fluctuate on an annual basis. We tested the model under different environmental conditions to examine the effect of environment on the interactions of host dynamics and disease risk. Results indicate that host dynamics reduce mean nymphal infection prevalence and increase the yearly amplitude of nymphal infection prevalence and the density of infected nymphs. Effects were nonlinear and patterns in the effect of dynamics on amplitude in nymphal infection prevalence varied across locations. These results highlight the importance of further study of the effect of communitiy dynamics on disease risk. This will involve the construction of further theoretical models and collection of robust field data to inform these models. With a more complete understanding of disease dynamics we can begin to better determine how to predict and manage disease risk using these models.

2 Introduction

Emerging infectious diseases present an ever-growing threat to human health, agriculture, and native flora and fauna [1–3]. In humans, around 75% of emerging diseases are wildlife zoonoses. These diseases cause millions of cases each year, and many new diseases are emerging or reemerging every year. Across species, diseases spread by vector organisms are the most common, and a growing proportion of new emerging diseases in humans are vector-borne [1, 2, 4, 5]. These disease systems involve complex dynamics between wildlife hosts, vector organisms, and the disease itself. The study of vector-borne diseases is of interest to many fields, including ecology, epidemiology, climatology, and many other disciplines.

A key problem is understanding how to predict and control the proliferation of vector-borne diseases. With the complexity of the different organisms involved in these diseases, they are best thought of as webs of different interacting species [3, 6]. Studying the community ecology of these disease systems is fundamental to understanding how they develop and spread. The community ecology of disease is a rapidly developing field, but still relatively in its infancy [3]. Much research has focused on "simpler" applications of community and population ecology, such as single host-parasite interactions. The tools of community ecology allow an understanding of the mechanisms leading to the particular community assemblages we see today and the dynamics that shape the systems across time and space, including the emergence and spread of vector-borne diseases [4, 5]. This has particular benefit in informing how host communities and parasite communities develop and interact between levels and different scales, from within the individual to across ecosystems.

In studies on vector-borne diseases, research has aimed to understand the impact of different species and species communities on disease risk [6–15]. The impact of host

and community dynamics on Lyme disease risk is fairly uncertain considering the known and widely implicated potential of these dynamics to have a significant impact on how *B. burgdorferi* flows through wildlife communities. Rodents in particular are known to serve as important reservoir hosts for *B. burgdorferi*, and populations of these species often undergo extreme fluctuations in density driven by resources, predators, and environmental effects [6, 16–18]. Other important host species undergo population dynamics and many species are subject to changing populations and extinctions as a result of human caused disturbances [6, 16]. Research has been equivocal in determining the effect of host dynamics on disease, showing no effect or an inconsistent effect [19–22]. Understanding this process will allow us to better understand how different systems experience disease risk, and inform how disease may vary regionally or as species extinctions and invasions develop.

Lyme disease is one of the most prominent wildlife vector-borne diseases impacting health in the United States, with estimates of as 476,000 cases per year [23]. Disease models of Lyme disease treat hosts as static parameter values, with only a few models investigating the impact of using dynamic population data, and none investigating the impact that dynamics have on this system [21, 24–27]. To investigate the impact of host dynamics on Lyme disease risk, we have created a mathematical model which simulates the flow of disease between a detailed tick population and a small community of hosts. To investigate the impact of host dynamics on the model, densities of the primary rodent host, mice, are varied on an annual basis. By changing the mean density and variation from the mean in a collection of simulations, we will use our model to explore the impact that simple host dynamics have on disease risk measures of the model for a range of possible scenarios. This model will direct future research into the effect of host dynamics and disease risk and highlight the need for the further development of models and empirical studies investigating this topic.

3 Results

3.1 Site-specific effects of variance

We examined model data grouped by simulations run with zero variance (constant mouse densities) or the entire range of variances (1-99 mice) (S1 Table). *DIN* and *DON* show similar patterns between groups, with the maximum and amplitude of each being much larger in simulations with variance than those with constant mouse density. Further analysis continued to show similar effects between *DIN* and *DON*, and *DIN* is of a more direct concern, so we will focus on results for *DIN* as a proxy for both. *NIP* metrics show lowered averages and medians for mean, min, and max *NIP*, and increased amplitude between variance and no variance groups. Minimum and maximum values remained constant for most *NIP* metrics.

Mean *DIN* shows a positive linear relationship with mean mouse density, and a variable relationship with variance, ranging from a positive and slightly nonlinear relationship at low means to a negative and slightly non-linear relationship at high density (Fig 1A). Similar positive relationships with variance and mean mouse density are demonstrated for amplitude, minimum, and maximum *DIN* (Figs 2A and 3A).

Fig 1. Response of mean density of infected nymphs and nymphal infection prevalence to variance in the mouse population and mean mouse density. A) shows the response of mean *DIN* to mouse variation and mean density. The relationship to mean mouse density is positive and linear, while the relationship to variance is weakly nonlinear, and shifts from a positive relationship to a negative relationship at low or high mean density, respectively. Contour lines plotted on the variance $\times$ mean plane and coloring reveal surface features. B) shows the response of mean *NIP* to mouse variation and mean density. The relationship between mean *NIP* and mean mouse density is a positive saturating curve

under low variation in the mouse population, which becomes a near linear relationship for high variance. The relationship between variance and *NIP* is negative, with higher variance decreasing *NIP* at the given mean mouse density. At low mean densities, very high variance begins to slow this decrease and even reverse it. Contour lines and coloration again reveal surface features.

Fig 2. Response of amplitude in density of infected nymphs and nymphal infection prevalence to variance in the mouse population and mean mouse density. A) shows the response of amplitude in *DIN* to mouse variation and mean density. The relationship to mean mouse density is positive and linear, while the relationship to mouse variance appears close to linear and is positive. Contour lines plotted on the variance $\times$ mean plane and coloring reveal surface features. B) shows the response of amplitude in *NIP* to mouse variation and mean density. The relationship between *NIP* and mean mouse density is a positive saturating curve under low variation in the mouse population, which becomes linear as variance increases. The relationship is a positive saturating curve between variance and amplitude in *NIP*. At high mean densities the relationship to variance is near linear, and shows signs of beginning to become negative at very high means and variances. Contour lines and coloration again reveal surface features.

Fig 3. Response of minimum density of infected nymphs and nymphal infection prevalence to variance in the mouse population and mean mouse density. A) shows the response of minimum *DIN* to mouse variation and mean density. The relationship to mean mouse density is positive and linear, while the relationship to mouse variance appears weakly nonlinear, and shifts from a slight positive relationship at low mean density to a slight negative relationship at high mean density. Contour lines plotted on the variance $\times$ mean plane and coloring reveal surface features. B) shows the response of minimum *NIP* to mouse variation and mean density. There is a nonlinear positive relationship between minimum *NIP* and mean mouse density. The relationship between variance and minimum

NIP is negative, with higher variance decreasing minimum *NIP* at the given mean mouse density. At low mean densities, very high variance shows the slightest sign of beginning to increase the minimum *NIP*. Contour lines and coloration again reveal surface features.

Measures for *NIP* show nonlinear relationships with both mean mouse density and variance. These measures are positively related with mean mouse density (Figs 1B, 2B, and 3B). At low variance this relationship is a saturating curve, while with higher variance this relationship becomes linear. Mean *NIP* decreases with variance, but high variance at low means begins to slow and eventually reverse this decrease (Fig 1B). The minimum point of this shift changes to higher variance as the mean mouse density increases, with no minimum appearing in the range of explored variances for higher mean densities. The amplitude of *NIP* follows a saturating curve across variance levels, reaching a maximum and decreasing for high variance and high mean mouse density (Fig 2B). The minimum *NIP* shows a strong negative response to variance (Fig 3B), while the maximum shows an unclear and relatively weak effect (S1 Fig), with a slight positive relationship at low mean mouse density shifting to a slightly negative relationship at high density.

The distributions of mean, minimum, and maximum *NIP* shows a negative shift in the median *NIP* measure with increasing variance, with this shift being strongest in minimum *NIP* (S1 Table). Median amplitude in *NIP* shows a positive shift with increasing variance (S1 Table). The median of mean and minimum *DIN* remains fairly stable, while amplitude and maximum *DIN* increase with variance (S1 Table). The median of mean *DIN* remains nearly constant, while amplitude *DIN* increases, and the median of minimum and maximum *DIN* decrease and increase, respectively with variance (S1 Table).

3.2 Effects of variance across variable weather inputs

We examined disease metrics across the selected locations to investigate patterns between sites and general geographic regions. *DIN* measures showed somewhat of an in-

crease in mean, minimum, and maximum *DIN* under warmer environmental conditions, but showed no discernible changes in the pattern of this effect. Mean, minimum, and maximum *NIP* across locations shows very similar effects of mouse population variance, with the range and interquartile range remaining similar while the median shifts down in response to variance. This effect is apparent between geographic regions as well, though regions differ in their distributions for both *DIN* and *NIP*. Amplitude of *DIN* has a consistent pattern between locations and regions with or without variance (Fig 4A). *NIP* amplitude has a markedly similar response to variance across locations and regions despite variability with stable host populations (Fig 4B).

Fig 4. Impact of variance in mouse population on amplitude of density of infected nymphs and nymphal infection prevalence under varying environmental conditions. A) displays the distributions of amplitude in *DIN* for locations with no variance or variance for medium variance levels ($\sigma = 33 - 67$). The left column shows boxplots for each location, while the right column shows boxplots for locations grouped by rough geographic area, with "West" indicating sites on the western range of Lyme disease and Eastern black-legged ticks. B) displays the same information for amplitude in *NIP*.

3.3 Sensitivity Analysis

Parameters for temperature induced activity and survival were important parameters for all measures of DIN, DON, and *NIP*. Parameters for maximum on-host survival of immature ticks and hardening nymphs and engorgement index also were correlated with disease measures. Weekly cumulative degree week thresholds also proved to be important, as well as parameters related to host survival rates.

4 Discussion

Host dynamics appear to have little effect on the density of infected ticks, while the proportion of infected ticks is affected. Our knowledge of the complexity of the species involved in these disease systems indicates that the study of host dynamics is important to our understanding of disease risk to humans. Yet, few studies have thoroughly investigated this. Here, we have investigated this possibility by developing a Lyme disease model which incorporates simulated host dynamics in rodent hosts, and investigating the impacts on disease risk predictions. The study of emerging infectious diseases continues to become more important as increasing numbers of diseases emerge or reemerge. Vector-borne diseases pose a particular threat with expanding ranges and the complex dynamics of spread.

4.1 Associations Between Host Dynamics and Disease Risk

Model results indicate that variance in the mouse population has only a small and inconsistent effect on mean *DIN* and *DON*. While somewhat counterintuitive, this result is not as surprising as it may seem. With the high association between small mammal density and *DIN* [16, 19], host density is a very reliable predictor of tick density. Tick density tracks host density, rising and falling in response to corresponding changes in the host population. The result is that mean tick density trends to the average expected from the mean host density in the model. Modeling studies have demonstrated that incorporating long-term empirical data on host density yields more accurate predictions of tick density when predicting disease risk at specific sites [21]. The effect on overall model output has not been determined, with research focusing on the qualitative accuracy of predictions on short timescales rather than multi-year simulations or investigation of model behavior. Studies that have considered host dynamics have focused solely on the effect of host density on disease risk rather than the effect of changing host density on disease dynamics. The results of

our model still align with this research, and demonstrate the direct impact of host density on *DIN* and *DON*.

Long term measurements of interannual variation in infection prevalence is lacking, and few modeling studies report yearly predicted *NIP* **e.g. ?????** [21]. Available results show little variation in mean *NIP* with a constant host population, while simulations incorporating field data on host populations demonstrate lowered and more variable *NIP*. Empirical studies demonstrate this same variability in annual *NIP*, [19, 28, 29] which our results align with. Studies which examine variation in the host population also focus on the predictive ability of host density for *NIP*. The density of small mammal hosts has been found to be a poor predictor of disease risk [16, 19]. On the other hand, resources such as acorns can be a good predictor of mean *NIP*. This likely results from direct changes in the proportion of competent host species in the system, e.g. seed predators. The density of hosts does not necessarily indicate changing host proportions, and may instead result from community-wide effects that change overall host density. In this model, we have demonstrated the scenario in which the proportion of competent hosts is changing by directly changing the density of a single host, and thus the proportional density, of hosts in the model system. The resulting effect on mean *NIP* is apparent in the results, and demonstrates the importance of considering relative host densities of competent and incompetent species rather than focusing on specific hosts or total host density in a system.

Results further show that the strength of host density variability is important, with a parabolic response of *NIP* to variance apparent in model results (Fig 1B). This likely results because all means $0-99$ mice$^{-ha^2}$ are simulated, and for each mean, variance from $0-99$ mice$^{-ha^2}$ is also simulated. For mean host densities < 99, the range of variance will overlap with 0 from $0-99$. Mouse density is bounded by 0, as negative density of course makes no sense. With greater variance the mean density of mice in a simulation will be higher than the mean of the distribution. The decrease of *NIP* in response to variance be-

gins to flatten out with boost in mouse density, and eventually even starts to increase *NIP* as the proportion of mice shifts. Figs 1-3 could rather show the relation between true simulated mouse density, variance, and *NIP*, but this neglects to show the nature of the response of *NIP* to variance at a simulated mean. The variance must exceed the mean mouse density before mean *NIP* begins to rise again (Fig 1B), showing that the high variance has a strongly negative effect on *NIP* that remains even after mean host density has been boosted significantly.

4.2 Temporal Dynamics in Disease Risk

In the model, what we have defined as amplitude serves as an indicator of the range of a disease measure, and thus disease risk, over the course of a year. This quantifies how variance and mean host density affects disease predictions in the model. A greater amplitude indicates greater contrast between least and most risky seasons, and a smaller range indicates similar risk between seasons. Understanding this range gives a sense of the pattern of disease as predicted by a model. The density of infected nymphs and total nymphs fluctuates seasonally, with both measures typically peaking in late spring or early summer to later in the year depending on how *DIN* is measured in a study. Changes in the amplitude of *DIN*/*DON* represent a change in the regular pattern of disease. The positive shift in amplitude for *DIN* shows a change in this pattern, and is a result of high host burdens supporting increased 'crops' of ticks in high host density years. The minimum unsurprisingly shifts very little, as this represents the sharp drop in tick densities as a result of mortality during periods of low activity and cold temperatures during the winter.

Intraannual variation data for *NIP* is very lacking, but the few studies that have been conducted indicate that seasonal *NIP* variability is indeed present in wild populations, and thus may present an important consideration when forecasting and managing disease risk through human behavioral changes [30, 31], and might also have value in sea-

sonally focused wildlife management and disease prediction [32]. Mathematical models of Lyme disease, which often operate on sub-yearly time scales, predict this seasonality. This behavior is a feature of modeled interactions between populations of susceptible and infected ticks and hosts, which fluctuate throughout the course of a year in response to host births, deaths, and infection rates, which are related to periods of tick activity. Our model shows that host variation affects the amplitude of *NIP* in a year. The minimum range of *NIP* was most strongly affected, which suggests that host variation may be important in determining the magnitude of periods of low and high risk, likely in response to changes in the birth/death ratio throughout a year. Prior modeling studies have suggested that co-occurrence of host density increases and high questing tick activity may boost tick density [32], but it is not known how this would affect *NIP*, and this was not explored in our model.

4.3 Varying Patterns in Disease Risk Under a Changing Environment

While this model is not intended to be predictive of the specific dynamics of a particular area, qualitative changes in the response to host dynamics under different environmental conditions are of interest. We used the environmental conditions of different geographic locations to explore this idea. Model results show a latitudinal gradient in the magnitude of *DIN* and the pattern of the response of *NIP*. The increase in *DIN* measures at locations with higher annual temperatures is expected, as warmer winters result in greater tick survival and activity. The consistency of the response between locations for most measures is rather surprising, and suggests that similar communities of species will have similar disease dynamics at different locations, though the disease risk may be different between sites. The changing pattern in the effect of variance on the amplitude of *NIP* at different locations, however, demonstrates the importance of considering host dynamics. It is

apparent that environmental conditions may alter how disease risk interacts with host density and host variance at different sites. Incorporation of host dynamics should allow for greater understanding of the particular disease dynamics when forecasting disease risk at specific locations using mathematical models. Further study of how different kinds of host dynamics affects the prediction of disease risk will be valuable for better understanding our models of disease as well as patterns in disease under real world patterns of host dynamics.

4.4 Further Directions

Our results suggest that host dynamics, and more specifically the magnitude of variation in host population densities is as an important consideration when modeling Lyme disease. More research is needed to understand how these dynamics may affect the use of theoretical models as exploratory and predictive tools. This might include simple to detailed modeling of host dynamics, or direct use of long term population data. Predictive models should rely on either detailed modeling of host dynamics or, preferably, long-term host data to investigate location-specific disease dynamics. This will allow these models to more accurately describe disease at specific locations and will further the use of theoretical studies as investigative tools for management of disease risk.

In our model, we assume instantaneous births at the beginning of a year, which will impact the ratio of infected to susceptible hosts when the host density is increasing. While this is a biologically unrealistic scenario, it presents a situation in which this shift in infected host prevalence drops as a result of reproduction, one of the important ways by which host dynamics are likely to impact disease risk, and especially the prevalence of infection. Any process that significantly shifts the proportion of susceptible hosts is likely to have repercussions on disease dynamics. This might occur in the real world as a result of normal population dynamics such as overwintering deaths in host species, seasonal periods of reproduction, or as a result of increased resource levels. In future models, host population

dynamics might be modeled on a shorter timescale, reflecting seasonal birth and death rates or the response to resource levels such as seed masting.

An important point to investigate is how the density of hosts in one year impacts disease measures in successive years in a host dynamics simulation. This can be explored using current model data to investigate how the relationship between host density and disease changes at different host variance levels. It will also be important to determine how the timing of host population changes might affect the timing of peaks in disease risk. It has been shown that this can affect tick density [32], but the interactions of patterns in host density with *DIN* and *NIP* have not been explored. This can be examined in our model by changing the week in which the new mouse population is chosen or by introducing a more complex model of mouse population dynamics. As has been suggested with *DON* and the interaction between host density and tick density peaks, the timing of tick activity, questing, and life stage peaks is likely to factor into further layers by which hosts may influence disease dynamics.

This project has demonstrated the importance of considering population dynamics in tick hosts when modeling Lyme disease. This model only begins to touch on potential outcomes on model behavior with the incorporation of very simple host dynamics. Potential avenues of expansion and further exploration with this model are many, and they offer strong potential to further our understanding of Lyme disease. With a complete understanding of how host, tick, and disease dynamics interact, we can begin to understand when and when not to emphasize different pieces of this complex system. Further exploration of the impact of host dynamics on disease risk will hopefully increase our knowledge of how Lyme disease spreads and behaves, and aide the development of models which are able to more accurately study and predict disease risk.

5 Methods

5.1 Tick Population Structure

The model consists of a collection of discrete-time difference equations representing the populations of a tick species and three hosts (S1 File). The tick population is stage structured and details each of the main life stages and substages through which an *Ixodid* tick will evolve (Fig 5, S2 Table).

Fig 5. Flow of ticks through different developmental stages and infection. The structure and flow of the tick population through different developmental stages is shown. Infected ticks go through the same stages but are kept as a separate population. Infection occurs during blood meals on hosts, which can transmit to and from ticks and their hosts. New eggs from infected and uninfected adults produce the next generation of uninfected ticks.

The tick population is highly detailed to ensure realistic dynamics in vector abundance and disease transmission. Ticks that enter a stage in a given week are tracked as a cohort and undergo the appropriate processes for that stage (Fig 5, S3 Table). Ticks of a stage in one week are a function of those that have survived from the previous week, with a gain or loss of density in one stage from development, survival, host finding, and infection of susceptible ticks.

The maximum time which a tick may spend in a life stage is unclear from laboratory [33, 34] and field studies [35–37], and models have incorporated a variety of assumptions to give life stage limits [21, 24, 25, 27]. We have set 52 weeks as a maximum limit that ticks of a cohort are tracked. We used cumulative degree weeks (CDW) to determine development rates between major life stages (egg, larvae, nymph, adult) as CDW has been shown to relate well to tick phenology and is a standard in many models [21, 25, 38, 39].

The cuticle hardening period undergone by free-living stages is a final point of confusion, with estimates ranging from 0-4 weeks, and some models only considering hardening in larvae. We have chosen a hardening period of one week for all free-living stages.

5.2 Host Population Structure

There are three hosts in the model: mice, a "medium" mammal species, and deer. Medium mammals and deer remain at constant densities of 4 and 0.4 ind. ha^{-1}, respectively. These values were selected from the literature to keep tick densities within that predicted by previous models and aide in potential comparisons [21]. Both species have a constant survival rate to provide lifespans of 2 and 3 years, respectively. This rate allows infection to “clear” from the population as offspring are assumed to be born susceptible. Mice have a clearing rate for a 1 year lifespan. Lifespans were estimated from literature for mice [40–42] and deer [43], and 2 years was chosen for medium mammals to provide a suitable intermediate host.

Mouse densities (M) are drawn from a normal distribution (N) to simulate population dynamics. Density values are bounded by zero, and by varying the mean (μ) and variance (σ^2) of the distribution a range of population dynamics can be simulated, including $\sigma^2 = 0$, or constant mouse density (Fig 6). For an increase in mice, the difference ($\pm\Delta_M$) is added to the population of susceptible (S) individuals, while a decrease proportionately affects both susceptible and infected (I) individuals.

Fig 6. Sample time series of model output with or without mouse variance. Data from two simulation runs are shown in the left and right columns, with a mean density of mice $\mu = 30$ individuals per hectare and zero variance ($\sigma = 0$) or a standard deviation of 25 individuals per hectare around this same mean. All other input and parameters remain the same. Shading indicates each segment of 52 weeks or one year. (a) and (d) show the total density of eggs and questing larvae, nymphs, and adults. As is apparent, the quest-

ing populations of nymphs and adults are significantly smaller than the total population of questing larvae, as most larvae do not manage to survive and find hosts. Populations fluctuate on an annual basis but with different phases. In (d) differences in density are apparent as a result of variable host populations. (b) and (e) show the populations of on host larvae, nymphs, and adults over time. Again, these densities cycle yearly, and changes in on host density are apparent with $\sigma = 25$ in (e). (c) and (f) demonstrate the difference in mouse density for a simulation without variation (c) and with variation (f) in mouse density. At the beginning of each year the population of mice is changed via a random distribution.

$$M_{y+1} = N(\mu, \sigma^2) \tag{2.2.1}$$

$$\Delta_M = M_{y+1} - (S_y + I_y) \tag{2.2.2}$$

$$S_{y+1} = S_y + \Delta_M, \quad \Delta_{\mathbf{M}} > \mathbf{0} \tag{2.2.3}$$

$$S_{y+1} = S_y + \Delta_M \times \frac{S_y}{S_y + I_y}, \quad I_{y+1} = S_y + \Delta_M \times \frac{S_y}{S_y + I_y}, \quad \Delta_{\mathbf{M<0}} \tag{2.2.4}$$

5.3 Activity and Host Finding

Questing ticks seek out hosts each week. The total rate at which hosts are found is determined by the host finding rate and the tick activity rate. The host finding rate (F_x) for a host species (x) is modeled as in other discrete-time tick models [21, 25] as this strategy yielded realistic rates of host finding for a sustained tick population. In Equation **??**, a is a host species and tick life stage (i) dependent coefficient, which relates the base finding rate of a tick to host density (H_x). The exponent of 0.515 scales down the rate of host finding to produce realistic densities [25]. The host finding rate is scaled via the level of tick activity, with F_x being the maximum host finding rate assuming 100% tick activity. Tick activity (A) is calculated with a normal distribution (N) centered on an optimal activity temperature

(t_{opt}), with a variance (σ^2), both determined from empirical measurements of activity levels across temperature [44, 45]. The final number of questing ticks (Q) which find a host x in a given week is the product of these rates and the total questing density. Each host species has a maximum host burden. If new questing ticks will cause hosts to exceed their burden in the successive week, ticks which exceed this threshold will remain in the questing population.

$$F_x = a_{i,x}(H_x)^{0.515} \tag{2.3.1}$$

$$A = N(t_{opt}, \sigma^2) \tag{2.3.2}$$

$$Q_x = F_x \cdot A \cdot Q \tag{2.3.3}$$

5.4 Survival

Eggs, questing, and engorged ticks exhibit environmentally dependent survival (S_e), modeled with normal distributions for temperature (T_s) and precipitation index (P_s). Optimal temperature (t_s) and precipitation index (p_s) values were chosen from the literature and the variance of distributions were adjusted to produce reasonable tick densities [21, 25, 35, 37]. This eliminates assumptions made in previous models, as exact relationships between environmental conditions and survival have not been determined.

$$T_s = N(t_s, \sigma^2), \quad P_s = N(p_s, \sigma^2) \tag{2.4.1}$$

$$S_e = T_s \cdot P_s \tag{2.4.2}$$

On-host ticks exhibit density dependent survival. Studies demonstrate this may result from true density dependence or from density dependent host grooming behaviors as a result of tick exposure. To implement this, an exposure index (EI) is calculated which measures the total number of ticks on each host type (x), scaled proportionately by mass

of each life stage for the previous 8 weeks, with a loss of exposure of 0.44 per week. For each host type and tick life stage, there are given estimated minimum and maximum survival rates for high and low exposure rates. In between these bounds, on-host survival is determined by Equation **??**, which yields a linear decrease in survival for increased EI.

$$EI = \sum_{i=1}^{9} 0.44^{i-1} \cdot (0.0021L_{(t-i)} + 0.014N_{(t-i)} + A_{(t-i)}) \tag{2.4.3}$$

$$S_o = \frac{S_{min} - S_{max}}{EI_{max} - EI_{min}} \cdot (EI - EI_{min}) + S_{max} \tag{2.4.4}$$

Ticks in the hardening stages are modeled with a constant survival, as molting success becomes the primary determinant of survival. Parameterization is based off of previous models to ensure realistic rates [21, 25].

5.5 Infection

Transmission occurs during the on-host stages, starting in larvae, and passes upwards through life stages, but will not transmit from adult ticks to eggs [46]. Ticks disperse evenly between infected and susceptible hosts of the same species, and the rate of infection from hosts to ticks is determined by the competency of each host species, the proportion of infected hosts of each species, and the density of ticks per host. Competency for mice is set to 75%, and deer to 0% [6, 13, 14, 19, 47]. The intermediate host serves as a generic species to maintain infection in the system in the absence of mice, and has a competency of 50%, in line with other small to medium sized mammal species [6, 13, 16].

Host infection is slightly more complicated. Infected ticks distribute evenly among hosts, but infected tick burdens may be in the range of only a few to no ticks per host throughout parts of the year. During these periods, it is expected that some hosts may have

several ticks while others have none. We used a modification of a method established previously [21] which uses a Monte Carlo simulation to predict the rate of host infection, given the number of infected ticks per host (ITH) and assuming an infection rate of 100%, which is then scaled by the expected infection rate of ticks. This calculation is made several hundred times to ensure a robust calculation for infected tick burdens from 0.01 to 7.5 ITH, the upper range of which is sufficient to provide $> 99.9\%$ chance of infection. The ITH is scaled by an infection rate of 0.9 to provide a 90% chance of infection per infected tick to host. For sufficiently high ITH there will be an effectively 100% infection rate.

5.6 Environmental Data

Average temperature and relative humidity are indicated as the most significant environmental factors which affect survival and development in *Ixodid* ticks [35–37, 48]. In the northeastern United States, where Lyme disease is most prevalent, humidity does not appear to play as significant a role, as humidity ranges do not typically fall outside of those optimal for tick survival [27]. As long term humidity data is less easily available, precipitation is sometimes used as a stand-in, which we have chosen to do. The average temperature is calculated as the average of the minimum and maximum temperature recordings for a day, and precipitation is calculated as an index, (PI), measured as $1/10\ th$ the current week's $(w+1)$ rainfall (R) in mm with a loss of 65% from the previous week's (w) index.

$$PI_{w+1} = R_{w+1} + 0.65PI_w \tag{2.6.1}$$

We obtained daily measurements of minimum and maximum temperature and precipitation from 22 sites throughout North America [49]. Data were selected to cover a range of locations and climate conditions from 1971-2021. Data were converted to weekly

461 measurements and mean temperature and precipitation indices were calculated. Portland,
462 Maine weather data was used as the primary location of focus for investigating model
463 behavior.

464 5.7 Simulation

465 All Simulations were run in Julia version 1.6.1 [50]. A variety of packages were
466 used in the process of conducting simulations, analyzing data, and plotting in Julia [51–60]
467 and in R [61–63]. To investigate the impact of host population dynamics on disease flow in
468 the model, 10,000 simulations were run with mean and variance of the density distribution
469 for all combinations of each variable ranging from $0 - 99$ in increments of 1. Ranges were
470 chosen to cover empirical measurements of density in the white-footed mouse, *Peromyscus*
471 *leucopus*, and potential variation in these densities [17]. Simulations were repeated for each
472 of the 22 chosen locations to investigate how changing environmental data affects model
473 behavior. Simulation output consists of weekly time-series data for all tick and host stage
474 classes within the model. A single simulation involves calculating the output of the discrete
475 difference equations at each time step of one week, and using these result to calculate
476 again for each successive time step until the completion of the desired number of weeks of
477 simulation. The result is the time series data as described above, stored in large matrices
478 for each life stage and host type.

479 5.8 Model Analysis

480 Analysis of model data was conducted in Julia version 1.6.1, and plotting con-
481 ducted with Julia and R version 4.0.5. To determine model prediction of disease risk, we
482 calculated the mean, minimum, and maximum densities of infected and susceptible nymphs
483 per year for the last 10 years of each simulation. These data were used to calculate standard

disease risk measures. The density of infected nymphs, *DIN* was calculated as the mean, minimum, and maximum density of questing infected nymphs over the course of a year, with minimum and maximum density not necessarily aligned with the density of questing susceptible and infected nymphs. Density of nymphs, *DON* was calculated as the mean, minimum, and maximum density of the combined population of susceptible and infected nymphs. Nymphal infection prevalence, *NIP* was calculated as the mean, minimum, and maximum measures of the infected population divided by the combined population of susceptible and infected nymphs. Amplitude is measured as the yearly minimum subtracted from the maximum for these disease metrics. The mean over 10 years for each metric was used when analyzing results.

We completed a sensitivity analysis to determine the sensitivity of results to particular variables. Parameters were varied with a one at a time approach across a range from -10% to 10% of the baseline value. Sensitivity was calulcated as the percent change in the output measures (as are described above) divided by percent change in the parameter. Portland, Maine environmental data was used as well as a constant mouse density of 50.

6 Acknowledgements

We would like to express gratitude to Allison K. Barner and Stephanie R. Taylor for their input and guidance on this project and previous manuscript versions. We also express gratitude to the Buck Lab for Climate and Environment at Colby College, the Student Special Project Fund, and the Colby College Summer Research Assistantship for providing funding for the completion of this project.

References

[1] Shuvankar Mukherjee. "Emerging infectious diseases: epidemiological perspective." In: *Indian journal of dermatology* 62.5 (2017), p. 459.

[2] Lauren G Shoemaker, Evelyn Hayhurst, Christopher P Weiss-Lehman, Alexander T Strauss, Anita Porath-Krause, Elizabeth T Borer, et al. "Pathogens manipulate the preference of vectors, slowing disease spread in a multi-host system." In: *Ecology letters* 22.7 (2019), pp. 1115–1125.

[3] Pieter TJ Johnson, Jacobus C De Roode, and Andy Fenton. "Why infectious disease research needs community ecology." In: *Science* 349.6252 (2015), p. 1259504.

[4] Bayissa Chala and Feyissa Hamde. "Emerging and re-emerging vector-borne infectious diseases and the challenges for control: a review." In: *Frontiers in Public Health* (2021), p. 1466.

[5] Kate E Jones, Nikkita G Patel, Marc A Levy, Adam Storeygard, Deborah Balk, John L Gittleman, et al. "Global trends in emerging infectious diseases." In: *Nature* 451.7181 (2008), pp. 990–993.

[6] Richard S Ostfeld, Taal Levi, Felicia Keesing, Kelly Oggenfuss, and Charles D Canham. "Tick-borne disease risk in a forest food web." In: *Ecology* 99.7 (2018), pp. 1562–1573.

[7] Sarah E Randolph and Andeew DM Dobson. "Pangloss revisited: a critique of the dilution effect and the biodiversity-buffers-disease paradigm." In: *Parasitology* 139.7 (2012), pp. 847–863.

[8] PTJ Johnson and DW Thieltges. "Diversity, decoys and the dilution effect: how ecological communities affect disease risk." In: *Journal of Experimental Biology* 213.6 (2010), pp. 961–970.

[9] Richard S Ostfeld and Felicia Keesing. "Biodiversity and disease risk: the case of Lyme disease." In: *Conservation biology* 14.3 (2000), pp. 722–728.

[10] Chelsea L Wood, Kevin D Lafferty, Giulio DeLeo, Hillary S Young, Peter J Hudson, and Armand M Kuris. "Does biodiversity protect humans against infectious disease?" In: *Ecology* 95.4 (2014), pp. 817–832.

[11] Josh Van Buskirk and Richard S Ostfeld. "Controlling Lyme disease by modifying the density and species composition of tick hosts." In: *Ecological Applications* 5.4 (1995), pp. 1133–1140.

[12] Taal Levi, Felicia Keesing, Robert D Holt, Michael Barfield, and Richard S Ostfeld. "Quantifying dilution and amplification in a community of hosts for tick-borne pathogens." In: *Ecological Applications* 26.2 (2016), pp. 484–498.

[13] Samniqueka J Halsey and James R Miller. "Maintenance of Borrelia burgdorferi among vertebrate hosts: a test of dilution effect mechanisms." In: *Ecosphere* 11.2 (2020), e03048.

[14] Kathleen LoGiudice, Richard S Ostfeld, Kenneth A Schmidt, and Felicia Keesing. "The ecology of infectious disease: effects of host diversity and community composition on Lyme disease risk." In: *Proceedings of the National academy of Sciences* 100.2 (2003), pp. 567–571.

[15] Felicia Keesing, J Brunner, S Duerr, Mary Killilea, K LoGiudice, K Schmidt, et al. "Hosts as ecological traps for the vector of Lyme disease." In: *Proceedings of the Royal Society B: Biological Sciences* 276.1675 (2009), pp. 3911–3919.

[16] Richard Ostfeld. *Lyme disease: the ecology of a complex system*. OUP USA, 2011, pp. 22–78.

[17] Susan P Elias, Jack W Witham, and Malcolm L Hunter. "Peromyscus leucopus abundance and acorn mast: population fluctuation patterns over 20 years." In: *Journal of Mammalogy* 85.4 (2004), pp. 743–747.

[18] Mahdi Aminikhah, Jukka T Forsman, Esa Koskela, Tapio Mappes, Jussi Sane, Jukka Ollgren, et al. "Rodent host population dynamics drive zoonotic Lyme Borreliosis and Orthohantavirus infections in humans in Northern Europe." In: *Scientific reports* 11.1 (2021), pp. 1–11.

[19] Richard S Ostfeld, Charles D Canham, Kelly Oggenfuss, Raymond J Winchcombe, and Felicia Keesing. "Climate, deer, rodents, and acorns as determinants of variation in Lyme-disease risk." In: *PLoS biology* 4.6 (2006), e145.

[20] Stephan Davis and E Calvet. "Fluctuating rodent populations and risk to humans from rodent-borne zoonoses." In: *Vector-Borne & Zoonotic Diseases* 5.4 (2005), pp. 305–314.

[21] Holly Gaff, Rebecca J Eisen, Lars Eisen, Robyn Nadolny, Jenna Bjork, and Andrew J Monaghan. "LYMESIM 2.0: an updated simulation of blacklegged tick (Acari: Ixodidae) population dynamics and enzootic transmission of Borrelia burgdorferi (Spirochaetales: Spirochaetaceae)." In: *Journal of Medical Entomology* 57.3 (2020), pp. 715–727.

[22] Clive G Jones, Richard S Ostfeld, Michele P Richard, Eric M Schauber, and Jerry O Wolff. "Chain reactions linking acorns to gypsy moth outbreaks and Lyme disease risk." In: *Science* 279.5353 (1998), pp. 1023–1026.

[23] Center for Disease Control and Prevention. "Data and Surveillance." In: *National Center for Emerging and Zoonotic Infectious Diseases (NCEZID), Division of Vector-Borne Diseases (DVBD)* (2022). URL: `https://www.cdc.gov/lyme/datasurveillance/`

index.html?CDC_AA_refVal=https%5C%3A%5C%2F%5C%2Fwww.cdc.gov%5C%2Flyme%5C%2Fstats%5C%2Findex.html.

[24] NH Ogden, M Bigras-Poulin, CJ O'callaghan, IK Barker, LR Lindsay, A Maarouf, et al. "A dynamic population model to investigate effects of climate on geographic range and seasonality of the tick Ixodes scapularis." In: *International journal for parasitology* 35.4 (2005), pp. 375–389.

[25] GA Mount, DG Haile, and E Daniels. "Simulation of blacklegged tick (Acari: Ixodidae) population dynamics and transmission of Borrelia burgdorferi." In: *Journal of medical entomology* 34.4 (1997), pp. 461–484.

[26] GA Mount, DG Haile, and E Daniels. "Simulation of management strategies for the blacklegged tick (Acari: Ixodidae) and the Lyme disease spirochete, Borrelia burgdorferi." In: *Journal of Medical Entomology* 34.6 (1997), pp. 672–683.

[27] Dorothy Wallace, Vardayani Ratti, Anita Kodali, Jonathan M Winter, Matthew P Ayres, Jonathan W Chipman, et al. "Effect of rising temperature on Lyme disease: Ixodes scapularis population dynamics and Borrelia burgdorferi transmission and prevalence." In: *Canadian Journal of Infectious Diseases and Medical Microbiology* 2019 (2019).

[28] Sarah A Hamer, Jean I Tsao, Edward D Walker, and Graham J Hickling. "Invasion of the Lyme disease vector Ixodes scapularis: implications for Borrelia burgdorferi endemicity." In: *Ecohealth* 7.1 (2010), pp. 47–63.

[29] Eliza AH Little, John F Anderson, Kirby C Stafford III, Lars Eisen, Rebecca J Eisen, and Goudarz Molaei. "Predicting spatiotemporal patterns of Lyme disease incidence from passively collected surveillance data for Borrelia burgdorferi sensu lato-infected Ixodes scapularis ticks." In: *Ticks and tick-borne diseases* 10.5 (2019), pp. 970–980.

[30] Per Moestrup Jensen and Flemming Frandsen. "Temporal risk assessment for Lyme borreliosis in Denmark." In: *Scandinavian Journal of Infectious Diseases* 32.5 (2000), pp. 539–544.

[31] Catherine Bouchard, Cécile Aenishaenslin, Erin E Rees, Jules K Koffi, Yann Pelcat, Marion Ripoche, et al. "Integrated social-behavioral and ecological risk maps to prioritize local public health responses to Lyme disease." In: *Environmental Health Perspectives* 126.4 (2018), p. 047008.

[32] Hsiao-Hsuan Wang, WE Grant, PD Teel, and SA Hamer. "Simulation of climate-tick-host-landscape interactions: Effects of shifts in the seasonality of host population fluctuations on tick densities." In: *Journal of Vector Ecology* 40.2 (2015), pp. 247–255.

[33] Katherine M Kocan, José de la Fuente, and Lisa A Coburn. "Insights into the development of Ixodes scapularis: a resource for research on a medically important tick species." In: *Parasites & vectors* 8.1 (2015), pp. 1–6.

[34] Danielle R Troughton and Michael L Levin. "Life cycles of seven ixodid tick species (Acari: Ixodidae) under standardized laboratory conditions." In: *Journal of medical entomology* 44.5 (2007), pp. 732–740.

[35] NH Ogden, LR Lindsay, G Beauchamp, D Charron, A Maarouf, CJ O'callaghan, et al. "Investigation of relationships between temperature and developmental rates of tick Ixodes scapularis (Acari: Ixodidae) in the laboratory and field." In: *Journal of medical entomology* 41.4 (2004), pp. 622–633.

[36] Jesse L Brunner, Mary Killilea, and Richard S Ostfeld. "Overwintering survival of nymphal Ixodes scapularis (Acari: Ixodidae) under natural conditions." In: *Journal of Medical Entomology* 49.5 (2014), pp. 981–987.

[37] L Robbin Lindsay, Ian K Barker, Gordon A Surgeoner, Scott A McEwen, Terry J Gillespie, and Jeffrey T Robinson. "Survival and development of Ixodes scapularis (Acari: Ixodidae) under various climatic conditions in Ontario, Canada." In: *Journal of medical entomology* 32.2 (1995), pp. 143–152.

[38] Taal Levi, Felicia Keesing, Kelly Oggenfuss, and Richard S Ostfeld. "Accelerated phenology of blacklegged ticks under climate warming." In: *Philosophical Transactions of the Royal Society B: Biological Sciences* 370.1665 (2015), p. 20130556.

[39] NH Ogden, A Maarouf, IK Barker, M Bigras-Poulin, LR Lindsay, MG Morshed, et al. "Climate change and the potential for range expansion of the Lyme disease vector Ixodes scapularis in Canada." In: *International journal for parasitology* 36.1 (2006), pp. 63–70.

[40] Malcolm D Schug, Stephen H Vessey, and Andrew I Korytko. "Longevity and survival in a population of white-footed mice (Peromyscus leucopus)." In: *Journal of Mammalogy* 72.2 (1991), pp. 360–366.

[41] RW Steger, JJ Peluso, HH Huang, CA Hodson, FC Leung, J Meites, et al. "Effects of advancing age on the hypothalamic-pituitary-ovarian axis of the female white-footed mouse (Peromyscus leucopus)." In: *Experimental aging research* 6.4 (1980), pp. 329–339.

[42] Mark A Suckow, Karla A Stevens, and Ronald P Wilson. *The laboratory rabbit, guinea pig, hamster, and other rodents*. Academic Press, 2012.

[43] Anthony J DeNicola, Kurt C VerCauteren, Paul D Curtis, and Scott E Hyngstrom. *Managing white-tailed deer in suburban environments*. Cornell Cooperative Extension, 2000.

[44] Nicholas H Ogden, Genevieve Pang, Howard S Ginsberg, Graham J Hickling, Russell L Burke, Lorenza Beati, et al. "Evidence for geographic variation in life-cycle processes affecting phenology of the Lyme disease vector Ixodes scapularis (Acari: Ixodidae) in the United States." In: *Journal of medical entomology* 55.6 (2018), pp. 1386–1401.

[45] Stephen G Vail and Gary Smith. "Vertical movement and posture of blacklegged tick (Acari: Ixodidae) nymphs as a function of temperature and relative humidity in laboratory experiments." In: *Journal of Medical Entomology* 39.6 (2002), pp. 842–846.

[46] Lindsay Rollend, Durland Fish, and James E Childs. "Transovarial transmission of Borrelia spirochetes by Ixodes scapularis: a summary of the literature and recent observations." In: *Ticks and tick-borne diseases* 4.1-2 (2013), pp. 46–51.

[47] Christina M Parise, Nicole E Breuner, Andrias Hojgaard, Lynn M Osikowicz, Adam J Replogle, Rebecca J Eisen, et al. "Experimental demonstration of reservoir competence of the white-footed mouse, Peromyscus leucopus (Rodentia: Cricetidae), for the Lyme disease spirochete, Borrelia mayonii (Spirochaetales: Spirochaetaceae)." In: *Journal of medical entomology* 57.3 (2020), pp. 927–932.

[48] Christopher D Heaney, Katherine A Moon, Richard S Ostfeld, Jonathan Pollak, Melissa N Poulsen, Annemarie G Hirsch, et al. "Relations of peri-residential temperature and humidity in tick-life-cycle-relevant time periods with human Lyme disease risk in Pennsylvania, USA." In: *Science of The Total Environment* 795 (2021), p. 148697.

[49] Yuchuan Lai and David Dzombak. "Compiled historical daily temperature and precipitation data for selected 210 U.S. cities." In: (Jan. 2022). DOI: 10.1184/R1/7890488.v5. URL: https://kilthub.cmu.edu/articles/dataset/Compiled_

daily_temperature_and_precipitation_data_for_the_U_S_cities/7890488.

[50] Jeff Bezanson, Alan Edelman, Stefan Karpinski, and Viral B Shah. "Julia: A fresh approach to numerical computing." In: *SIAM review* 59.1 (2017), pp. 65–98. URL: https://doi.org/10.1137/141000671.

[51] Christopher Rackauckas and Qing Nie. "DifferentialEquations.jl – A Performant and Feature-Rich Ecosystem for Solving Differential Equations in Julia." In: *The Journal of Open Research Software* 5.1 (2017). https://app.dimensions.ai/details/publication/pub.1085583166 and http://openresearchsoftware.metajnl.com/articles/10.5334/jors.151/galley/245/download/. DOI: 10.5334/jors.151.

[52] James Fairbanks Seth Bromberger and contributors. *JuliaGraphs/LightGraphs.jl: an optimized graphs package for the Julia programming language*. 2017. DOI: 10.5281/zenodo.889971. URL: https://doi.org/10.5281/zenodo.889971.

[53] Mathieu Besançon. *VertexSafeGraphs.jl*. https://github.com/matbesancon/VertexSafeGraphs.jl. Version v0.1.0. May 2019.

[54] Patrick Kofod Mogensen and Asbjørn Nilsen Riseth. "Optim: A mathematical optimization package for Julia." In: *Journal of Open Source Software* 3.24 (2018), p. 615. DOI: 10.21105/joss.00615.

[55] Christopher Rackauckas and Qing Nie. "Adaptive methods for stochastic differential equations via natural embeddings and rejection sampling with memory." In: *Discrete and continuous dynamical systems. Series B* 22.7 (2017), p. 2731.

[56] Claus Fieker, William Hart, Tommy Hofmann, and Fredrik Johansson. "Nemo/Hecke: Computer Algebra and Number Theory Packages for the Julia Programming Language." In: *Proceedings of the 2017 ACM on International Symposium on Symbolic*

and Algebraic Computation. ISSAC '17. New York, NY, USA: ACM, 2017, pp. 157–164. DOI: 10.1145/3087604.3087611. URL: https://doi.acm.org/10.1145/3087604.3087611.

[57] Steven G. Johnson. *QuadGK.jl: Gauss–Kronrod integration in Julia*. https://github.com/JuliaMath/QuadGK.jl.

[58] Matteo Frigo and Steven G. Johnson. "The Design and Implementation of FFTW3." In: *Proceedings of the IEEE* 93.2 (2005). Special issue on "Program Generation, Optimization, and Platform Adaptation", pp. 216–231. DOI: 10.1109/JPROC.2004.840301.

[59] Mathieu Besançon, Theodore Papamarkou, David Anthoff, Alex Arslan, Simon Byrne, Dahua Lin, et al. "Distributions.jl: Definition and Modeling of Probability Distributions in the JuliaStats Ecosystem." In: *Journal of Statistical Software* 98.16 (2021), pp. 1–30. ISSN: 1548-7660. DOI: 10.18637/jss.v098.i16. URL: https://www.jstatsoft.org/v098/i16.

[60] Dahua Lin, John Myles White, Simon Byrne, Douglas Bates, Andreas Noack, John Pearson, et al. *JuliaStats/Distributions.jl: a Julia package for probability distributions and associated functions*. 2019. DOI: 10.5281/zenodo.2647458. URL: https://doi.org/10.5281/zenodo.2647458.

[61] R Core Team. *R: A Language and Environment for Statistical Computing*. R Foundation for Statistical Computing. Vienna, Austria, 2021. URL: https://www.R-project.org/.

[62] Hadley Wickham. *stringr: Simple, Consistent Wrappers for Common String Operations*. R package version 1.4.0. 2019. URL: https://CRAN.R-project.org/package=stringr.

[63] Karline Soetaert. *plot3D: Plotting Multi-Dimensional Data*. R package version 1.4. 2021. URL: https://CRAN.R-project.org/package=plot3D.

7 Supporting Information

S1 Fig. Response of maximum density of infected nymphs and nymphal infection prevalence to variance in the mouse population and mean mouse density. A) shows the response of maximum *DIN* to mouse variation and mean density. The relationship to mean mouse density is positive and linear, as is the relationship to mouse variance. Contour lines plotted on the variance $\times$ mean plane and coloring reveal surface features. B) shows the response of maximum *NIP* to mouse variation and mean density. There is a nonlinear positive relationship between maximum *NIP* and mean mouse density. The relationship between mouse population variance and maximum *NIP* is inconsistent, with higher variance increasing maximum *NIP* at the low mean mouse density. At higher mean densities, maximum *NIP* transitions to decreasing with variance. Contour lines and coloration again reveal surface features.

S1 Table. Summary Statistics, Grouped by Variance, DIN, NIP This table presents summary statistics for disease risk metrics, grouped by different levels of mouse population variance.

S2 Table. Tick life stages. Tick life and developmental stages represented in the model.

S3 Table. Demographic Tick Processes. Tick demographic processes represented in the model.

S4 Table. Parameters used in the model.

S5 Table. Parameters used in the model, continued.

S1 File. Model equations. The equations representing tick, host, and infection processes in the model are presented here. See S4 and S4 Tables for parameter names and purposes.

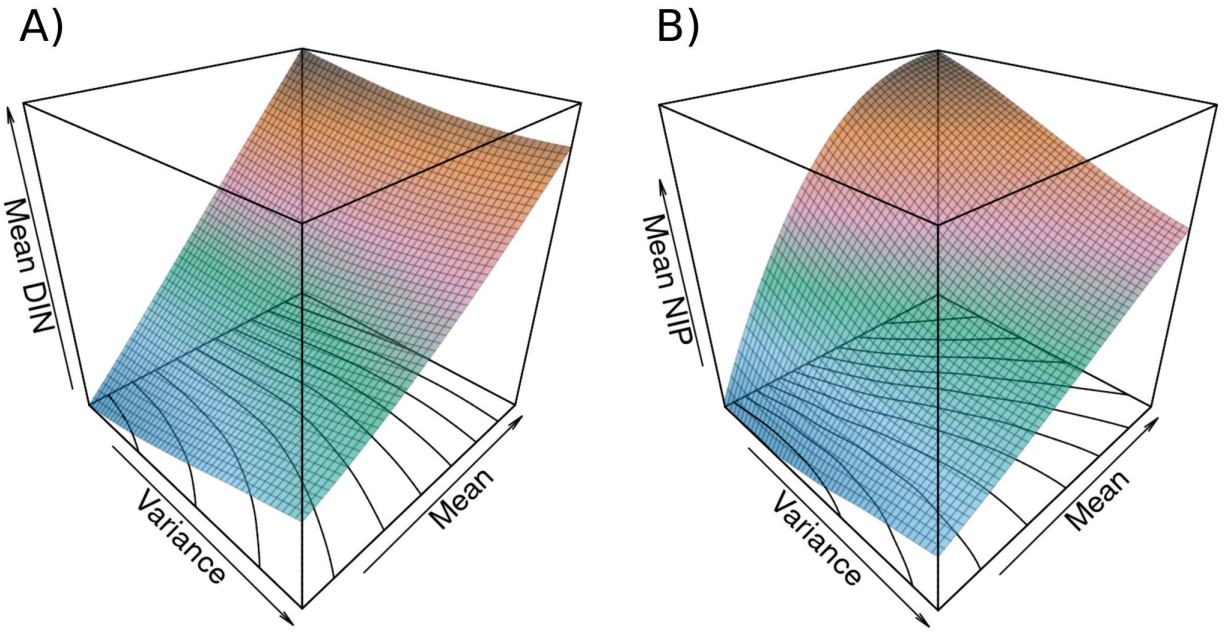
A)
Mean DIN
Variance
Mean
B)
Mean NIP
Variance
Mean

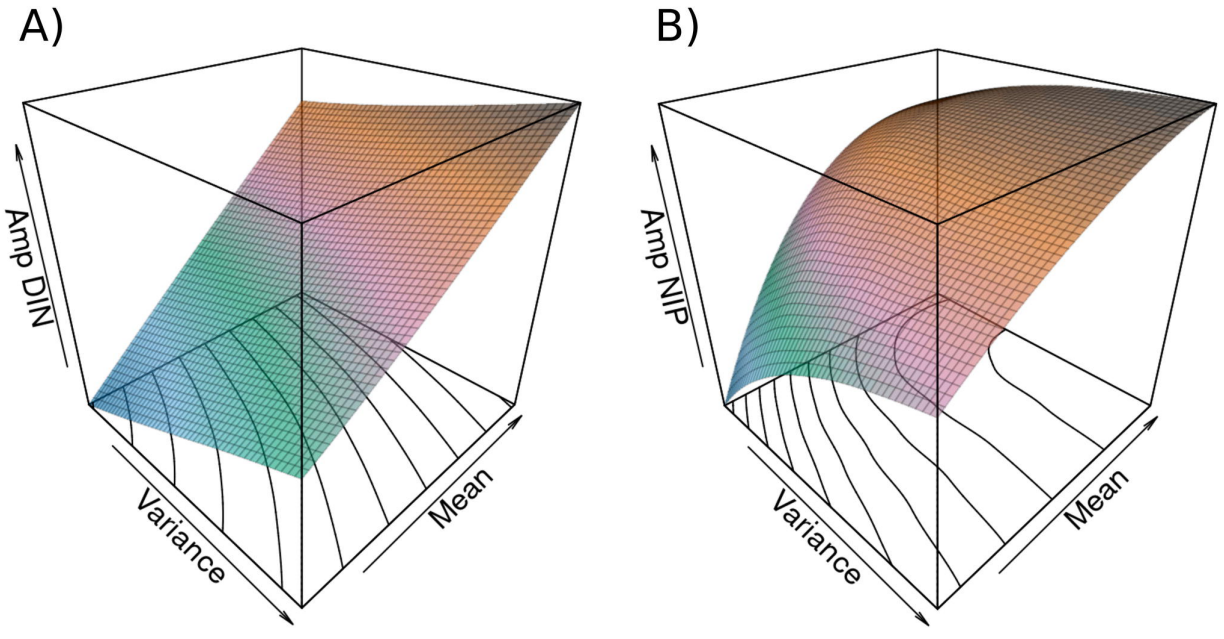
A)
Amp DIN
Variance
Mean
B)
Amp NIP
Variance
Mean

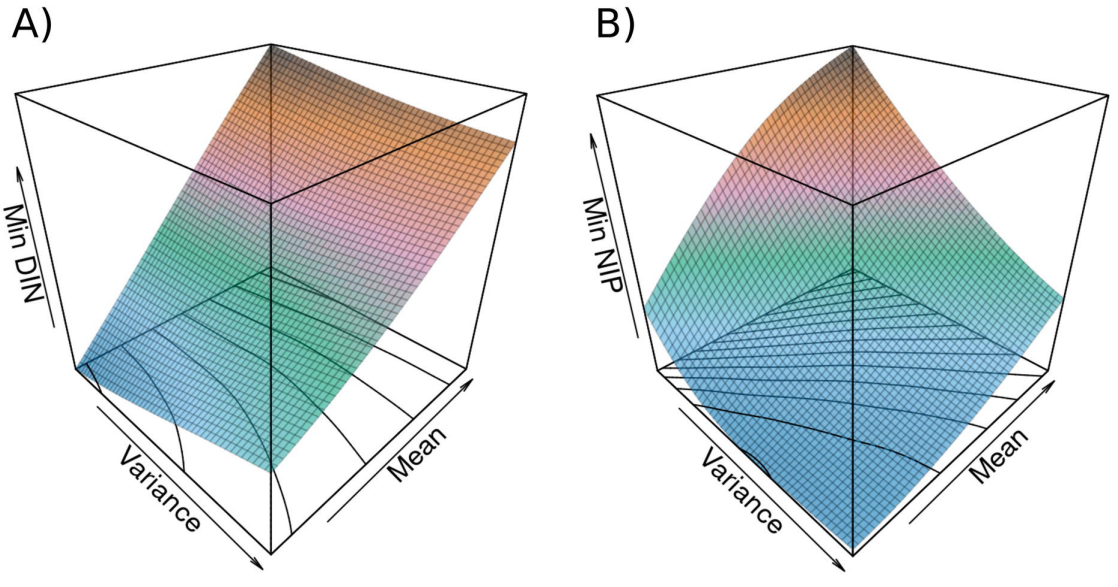
A)
Min DIN
Variance
Mean
B)
Min NIP
Variance
Mean

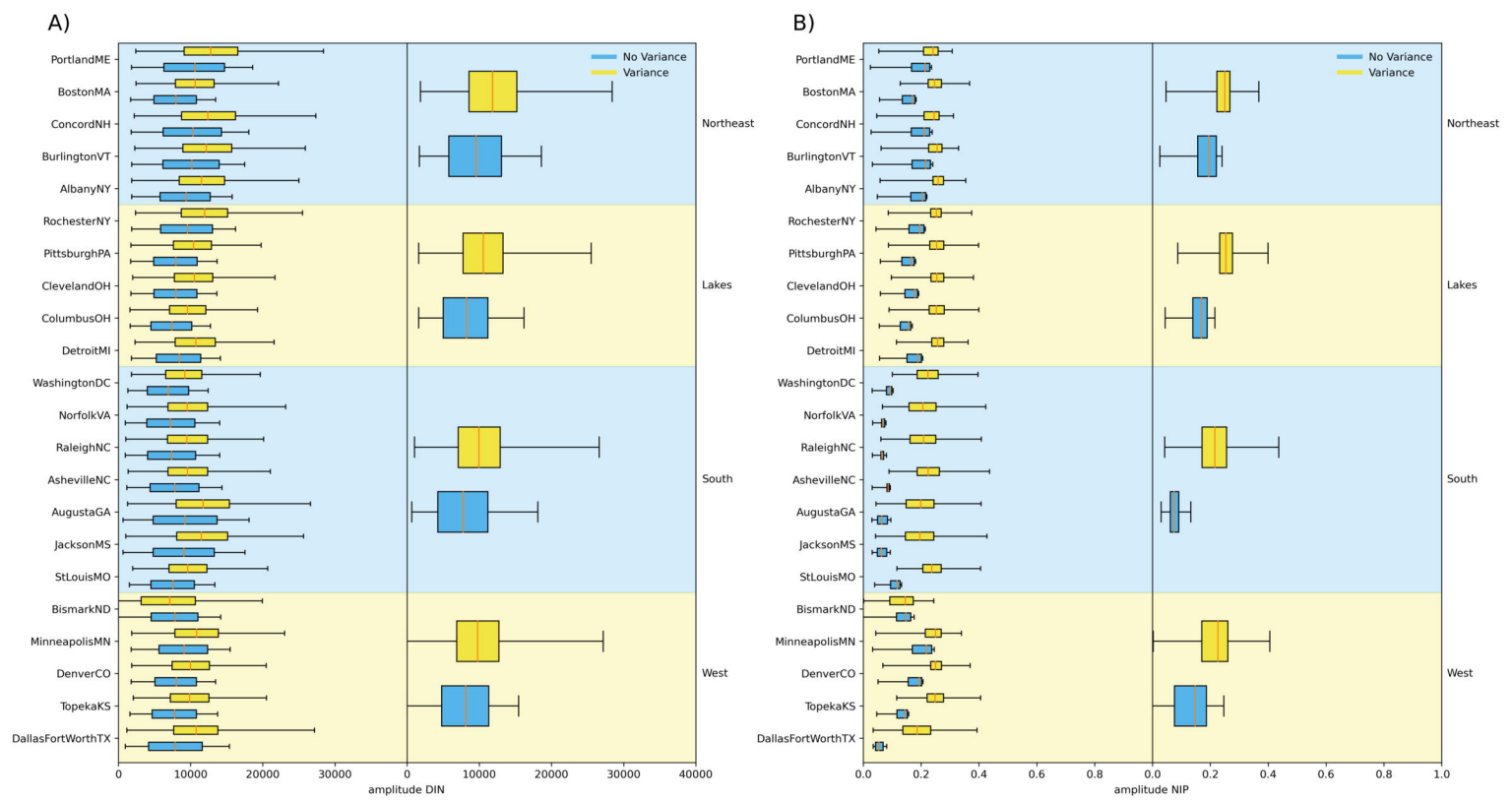
A)
B)
No Variance
Variance
PortlandME
BostonMA
ConcordNH
BurlingtonVT
AlbanyNY
RochesterNY
PittsburghPA
ClevelandOH
ColumbusOH
DetroitMI
WashingtonDC
NorfolkVA
RaleighNC
AshevilleNC
AugustaGA
JacksonMS
StLouisMO
BismarkND
MinneapolisMN
DenverCO
TopekaKS
DallasFortWorthTX
Northeast
Lakes
South
West
0
10000
20000
30000
40000
0.0
0.2
0.4
0.6
0.8
1.0
amplitude DIN
amplitude NIP

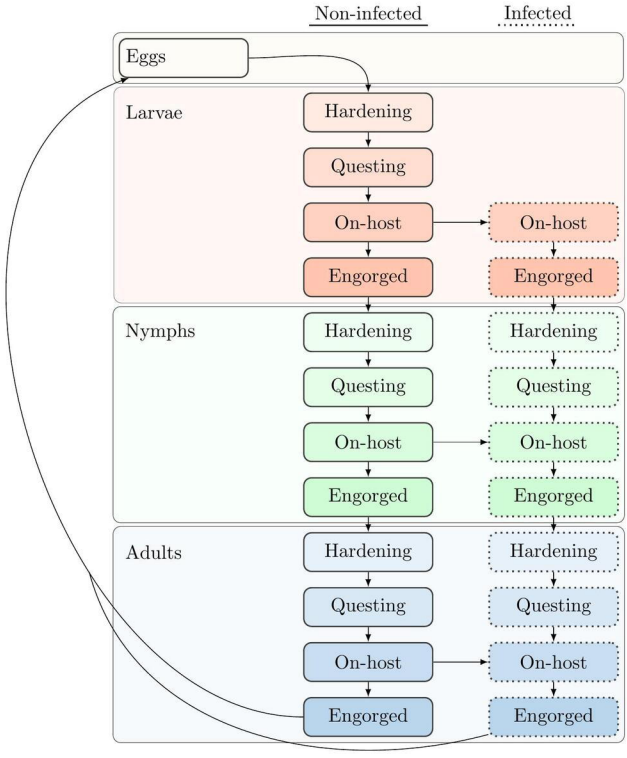
Non-infected
Infected
Eggs
Larvae
Hardening
Questing
On-host
On-host
Engorged
Engorged
Nymphs
Hardening
Hardening
Questing
Questing
On-host
On-host
Engorged
Engorged
Adults
Hardening
Hardening
Questing
Questing
On-host
On-host
Engorged
Engorged